

# Cascaded Single Photons from Pulsed Quantum Excitation

Juan Camilo López Carreño

*Institute of Theoretical Physics, University of Warsaw, ul. Pasteura 5, 02-093 Warsaw, Poland*

A two-level system is the most fundamental building block of matter. Its response to classical light is well known, as it converts pulses of coherent light into antibunched emission. However, recent theoretical proposals have predicted that it is advantageous to illuminate two-level systems with quantum light; i.e., the light emitted from another quantum system. However, those proposals were done considering continuous excitation of the source of light. Here, we advance the field by changing the paradigm of excitation: we use the emission of a two-level system, itself driven by a laser pulse, to excite another two-level system. Thus, we present a thorough analysis of the response of a two-level system under pulsed quantum excitation. Our result maintain the claim of the advantage of the excitation with quantum light, while also supporting the recent experimental observations of our system, and can be used as a roadmap for the future of light-matter interaction research.

## INTRODUCTION

Einstein's interest in the captivating interaction between light and matter brought his attention to the photoelectric effect [1], from which he established the quantized character of light. Later on, his research led him to the prediction of the process that we now refer to as *stimulated emission* [2]. Decades have passed, and we are still discovering new phenomena arising from light-matter interaction. In fact, it is one of the most fundamental areas of study for the advancement of quantum technologies [3–5]. Thus, every single day experiments are being carried out in a myriad of diverse condensed matter systems, including atomic ensembles [6–8], polaritons [9–13], phonons [14–16], plasmons [17–20], semiconductor quantum dots [21–24], perovskite crystals [25–28], transition metal dichalcogenides (TMDs) [29–33], hexagonal boron nitride ensembles [34–37], among many others. On the other hand, there is also a large set of light sources that could be used to excite the systems above. While on the early years of the field the illumination of the samples was done with lasers (or, in more modest laboratories, even with sodium lamps emitting thermal light), the observation of *antibunching* [38, 39] revolutionised the field. Now, the illumination toolbox includes a variety of more elaborated sources of light, including squeezed light [40–44], entangled photons [45–50], single photons [51–57],  $N$ -photon bundles [58] and, most recently, sources of quantum light, i.e., the light emitted from fundamental quantum systems [59–61]. All of these sources play an important role in the roadmap on quantum light spectroscopy [62].

Turning to the details of the implementations, there is also a divide between the experimental and theoretical approaches. Namely, an important consideration in experimental realizations is the mode of operation of the source of light, i.e., pulsed or continuous wave. The latter can be problematic, because during the time of excitation, the sample has no “off time” to cool down, and special care needs to be taken in order to avoid burning the sample. As a consequence, the intensity of the excitation is kept relatively low, thus narrowing down the range of accessible powers. Thus, usually when experiments involve exciting a system with light, the preferred method is to do it with pulsed sources. In fact, with this type of sources, one can better define wavepackets and discuss, e.g., correlations within

individual and among different wavepackets [63–65]. Furthermore, experimental techniques now allows the control over the duration and spectral properties [66] of the classical pulses, as well as the subsequent measurement of quantum emission [67] (even when various pulses with different lifetimes [68] are considered), the generation of entanglement using two pulses close in time to each other [69], and finally determining the fundamental limits of quantum light spectroscopy [70].

From a theoretical point of view, however, it is appealing to deal with continuous wave excitation, because it renders the Hamiltonian independent of time which, in turn, makes it possible to solve analytically the equations of motion of the system. Thus, apart from theoretical works devoted to reproduce particular observations [71, 72], and a recent comparison between the regimes that a semiconductor quantum dot can reach by being excited with continuous or pulsed light [73], and the description of the pulsed excitation of a quantum oscillator [74] and the mechanisms to describe them as a the interaction between a quantum dot embedded into a microcavity [75], the bulk of the theoretical corpus on this topic is based on continuous excitation.

In this manuscript, we present the description of the pulsed excitation of a fundamental block of condensed-matter, namely a two-level system (2LS). Furthermore, we use its emission to excite another 2LS, thus realising the so-called *cascaded excitation* with pulsed sources of quantum light. Given that both the mode of excitation (pulsed as compared to continuous) and the source of light considered (the quantum light emitted from the 2LS) are a novel addition to the literature, here we make a thorough description of the behaviour of the system: its one- and two-photon observables, such as the occupation and spectra; and second order correlation functions, respectively. Thus, while the results shown here are in agreement with the recent experimental realisation of this pulsed cascaded excitation [59], they also apply to the variety of platforms supporting two-level system analogues.

The rest of the paper is organised as follows: We begin with an overview of the recent experiment that motivates this study, and we introduce the theoretical formalism that describes the system as a whole. In particular, we define the quantum flux of the system which, as we shall see in the following pages, plays a fundamental role in the dynamics of the system and displays the most interesting behaviours. Next, we turn to the results,

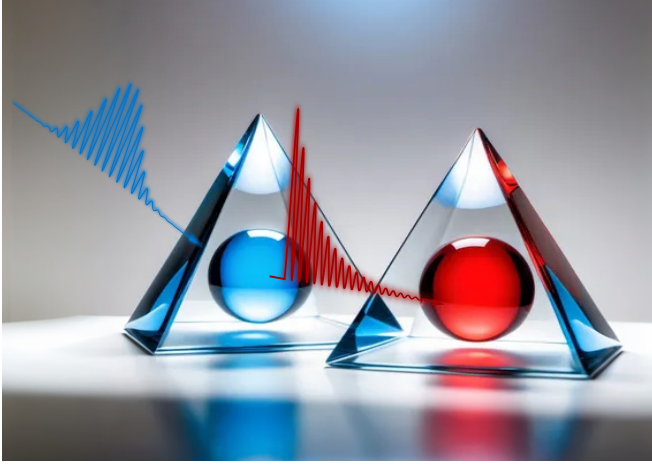


Figure 1. **Sketch of the cascaded excitation.** A classical pulse of light (blue line) is used to excite a two-level system, here depicted as a pyramid. The emission (red line) that comes out from the interaction of the 2LS with the classical pulse is collected and directed to an identical 2LS to excite it, this time with a pulse of quantum light.

starting with the one-photon observables, that is, the populations and the time-dependent emission spectra of the various components of the system; and ending with the two-photon observables, delving into the temporal structure of the emission as measured through the second-order coherence function. We then come to the end of our manuscript with a discussion of our results and the perspectives for impact in the field and future investigations.

## EXPERIMENTAL MOTIVATION

The theory for cascaded systems was introduced in the early 1990's [76, 77] to model experiments where microcavities were excited with squeezed light. Since then, theoretical studies have expanded the reach of the theory, by changing the source of light from classical to quantum, namely, the emission from a quantum system. The most fundamental system that one can use as a source is a two-level system. In fact, general considerations have been done around the excitation of bosonic [60] and fermionic [61] fields, showing that such a quantum excitation enables, e.g., unprecedented spectroscopic resolution [78], whereby the internal structure of the target of the excitation is probed with only two photons. Additionally, the cascaded theory has been used to explore fundamental topics, including chirality in non-hermitian systems [79, 80], the shaping of flying qubits [81], quantum steering [82]; but also to implement practical operations, such as feeding forward information into quantum reservoir networks [83–85].

However, despite the vast amount of theoretical developments done using the cascaded configuration to bring quantum states into quantum emitters, it was not until a few months ago that the technical capabilities of state-of-the-art experimental setups allowed for the actual implementation of such a cascaded excitation [59], thus measuring for the first time

the excitation of a quantum emitter with a pulse of quantum light [59].

Our experiment is divided in two stages: the first of them consists of the excitation of a quantum dot with the pulsed laser (cf. the blue line in Fig. 1); and the second one is the excitation of an identical quantum dot with the emission from the first one (which we have sketched as a red line in Fig. 1). Note that our experiment is based on the excitation of a quantum dot, but the theoretical description applies to any 2LS. Therefore, to keep the generality of the results, in the rest of the manuscript we will refer to the emitter as a 2LS instead of a quantum dot. Thus, the first stage is modelled through the Hamiltonian (we take  $\hbar = 1$  along the manuscript)

$$H_\sigma(t) = (\omega_\sigma - \omega_L)\sigma^\dagger\sigma + \frac{\Omega(t)}{2}(\sigma + \sigma^\dagger), \quad (1)$$

where  $\sigma$  is the annihilation operator associated to the 2LS (and which follows the pseudo-spin algebra). Here, we have also defined the natural frequency of the quantum dot  $\omega_\sigma$ , the frequency of the pulse laser  $\omega_L$ , and the time-dependent envelope of the pulse  $\Omega(t)$ . The dissipative character of the system is taken into account by upgrading the description to a master equation

$$\partial_t \rho = i[\rho, H_\sigma(t)] + \frac{\gamma_\sigma}{2}\mathcal{L}_\sigma(\rho), \quad (2)$$

where  $H_\sigma(t)$  is the Hamiltonian defined in Eq. (1),  $\mathcal{L}_c(\rho) = (2c\rho c^\dagger - c^\dagger c\rho - \rho c^\dagger c)$ , and  $\gamma_\sigma$  is the decay rate of the 2LS. Commonly, the envelope of the laser pulse has a Gaussian profile, given by

$$\Omega(t) = \frac{A}{\sqrt{2\pi}v^2} \exp\left[-\frac{(t-t_0)^2}{2v^2}\right], \quad (3)$$

which describes a pulse with integrated area  $A$ , centered at time  $t_0$  and with variance  $v^2$ , which is related to the full width at half maximum (FWHM) through the relation  $\mathcal{W} = 2\sqrt{2 \log 2}v$ .

In the second stage of the experiment, the emission of the 2LS goes away from the sample, meets a mirror, and comes back to re-excite the 2LS (cf. the Supplemental Material of Ref. [59] for the full description of the experimental setup). Thus, contrary to the case of the first stage of the experiment, here the 2LS is driven with quantum (rather than classical) light. Such an excitation is modelled as a cascaded system, where the emission from a 2LS (the source) is used to excite *another* identical 2LS (the target), as sketched in Fig. 1. Namely, the master equation of the whole experiment becomes

$$\begin{aligned} \partial_t \rho = i[\rho, H_\sigma(t) + H_\xi] + \frac{\gamma_\sigma}{2}\mathcal{L}_\sigma(\rho) + \frac{\gamma_\xi}{2}\mathcal{L}_\xi(\rho) - \\ - \sqrt{\chi_1\chi_2\gamma_\sigma\gamma_\xi} \{[\xi^\dagger, \sigma\rho] + [\rho\sigma^\dagger, \xi]\}, \quad (4) \end{aligned}$$

where  $H_\xi = (\omega_\xi - \omega_L)\xi^\dagger\xi$  is the Hamiltonian of the target quantum dot, which has decay rate  $\gamma_\xi$ , and the re-excitation is modelled through the ‘‘cascading’’ term in the second line. Rewriting the master equation (4) in the Lindblad form (see,

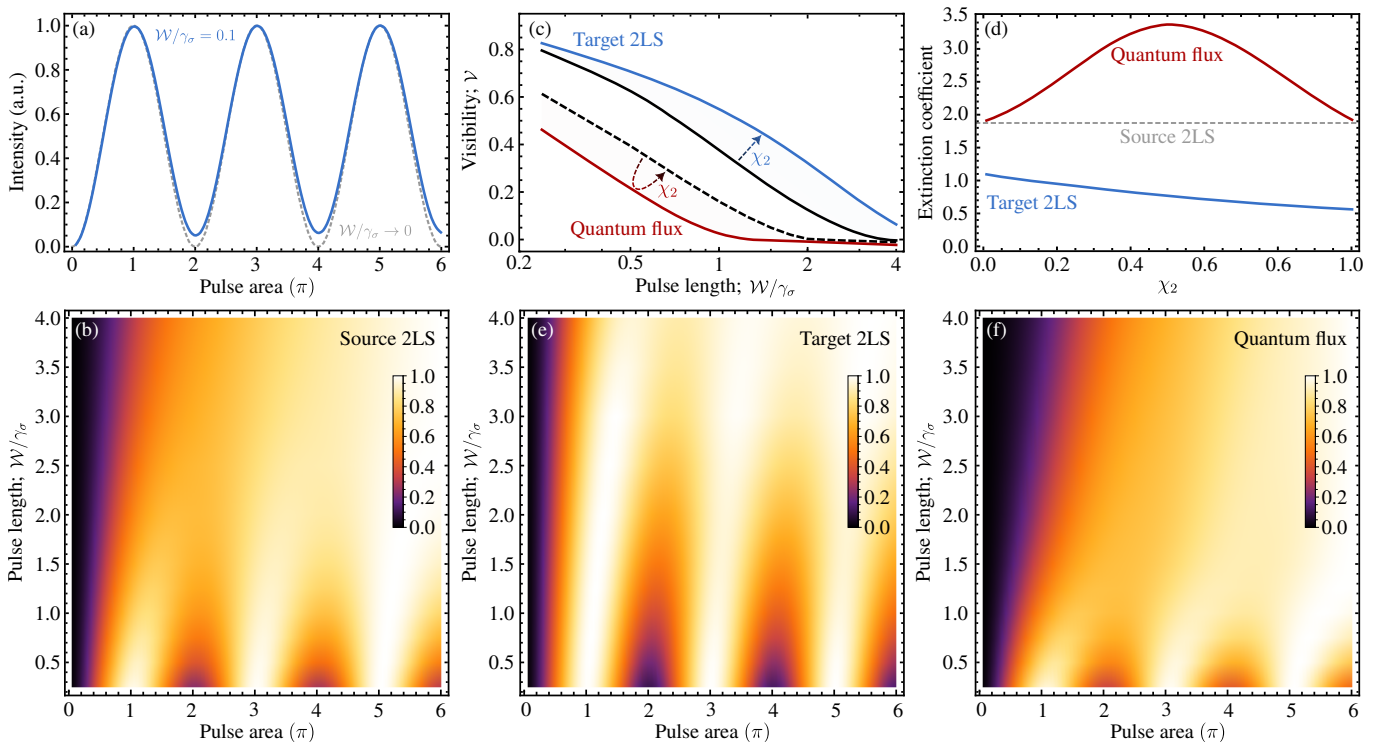


Figure 2. **Pulsed Rabi oscillations.** (a) Intensity of the emission from a 2LS pulsed with laser with vanishing (dashed) and finite but small (solid) length. (b) Intensity of the emission as a function of both the area and the length of the pulse, showing that the Rabi oscillations are quickly suppressed. (c) Visibility of the Rabi oscillations, as quantified by the normalized difference between the maximum near  $A = \pi$  and the minimum near  $A = 2\pi$ , for the source 2LS (dashed), the target 2LS (upper two lines, shaded in blue) and the quantum flux (lower two lines, shaded in red). For the latter two, the gradient indicates the variation of the parameter  $\chi_2$ . (d) Extinction coefficients for the visibility lines showed in panel (c), for the source 2LS (dashed), the target 2LS (blue) and quantum flux (red). (e, f) Same as in panel (b) but for the target 2LS and the quantum flux, respectively; calculated for  $\chi_2 = 1/2$ .

e.g., the Supplemental Material of Ref. [50] for the details), reveals that the two quantum dots are coupled dissipatively through a Lindblad superoperator  $\frac{1}{2}\mathcal{L}_{\mathcal{O}}(\rho)$ , where the operator  $\mathcal{O}$  is defined as

$$\mathcal{O} = \sqrt{\chi_1\gamma_\sigma}\sigma + \sqrt{\chi_2\gamma_\xi}\xi, \quad (5)$$

which, is commonly referred to as the *quantum flux* [86, 87] and, as we shall see in the following sections, induces a quantum interference which provides a mechanism to stimulated emission.

## RESULTS

### Pulsed Rabi Oscillations

The response of the classically excited 2LS as a function of the area of the laser pulse is well known [88]. Namely, For short-enough pulses, once the 2LS has interacted with the entirety of the pulse, the probability of finding the 2LS on its excited state is given by

$$P_e = \sin^2(A/2), \quad (6)$$

where  $A$  is the integrated area of the pulse. This is known as the area theorem.

Thus, one expects Rabi oscillations with unit visibility as a function of the area of the pulse, as shown in the dashed line in Fig. 2(a). However, although Eq. (6) is a good approximation for very short pulses, even for  $\mathcal{W}/\gamma_\sigma = 0.1$  we find a deviation from the perfect oscillatory behaviour [71, 72, 89, 90], as shown as a solid line Fig. 2(a). In fact, as the length of the pulse is increased, the oscillations become increasingly damped, up to the point in which the intensity of the light increases monotonically as a function of the pulse area. Such a behaviour is illustrated in Fig. 2(b), where we show the normalized intensity (for each pulse length) a function of the pulse area. There we can also see that, although for short pulses the position of the minima and maxima of the oscillations are given by odd- and even- $\pi$  pulses, respectively, as the length of the pulses increases, these positions start to drift away. Given that usually in experimental realisations of pulsed excitation the area of the pulse is not known, but instead it is inferred from the position of the minima and maxima of the Rabi oscillations, our observation provides an important warning.

Further, we can measure the visibility the oscillations, which we define as

$$\mathcal{V} \propto \frac{M_\pi - m_{2\pi}}{M_\pi + m_{2\pi}}, \quad (7)$$

where  $M_\pi$  is the maximum of the intensity around  $\pi$ -pulses,

and  $m_{2\pi}$  is the minimum of the intensity around  $2\pi$ -pulses. For the 2LS driven classically, the visibility of the oscillations is shown as a dashed line in Fig. 2(c), which displays an exponential decay as a function of the pulse length; namely, the visibility of the oscillations can be fitted as

$$\mathcal{V} = \exp(-\beta\mathcal{W}/\gamma_\sigma), \quad (8)$$

where  $\beta$  is the extinction coefficient, which for the source 2LS has the value  $\beta = 1.87$ . Notably, Fig. 2(c) shows that the oscillations are completely extinguished for pulses of length  $\mathcal{W}/\gamma_\sigma \geq 2$ .

We now turn to the Rabi oscillations of the 2LS driven with quantum light (i.e., the 2LS described with operator  $\xi$  in Eq. (4)), and the quantum flux (as defined in Eq. (5)), shown in Fig. 2(e) and Fig. 2(f), respectively. We find that the oscillations in the target 2LS are much more robust to the length of the classical pulse, remaining visible for pulses of up to four lifetimes of the 2LS; as shown in Fig. 2(c). The upper two lines show the visibility for  $\chi_2 \rightarrow 0$  (black) and  $\chi_2 \rightarrow 1$  (blue), and the color gradient indicates the variation of the parameter of incoherent coupling  $\chi_2$ . For the quantum flux, on the contrary, the visibility of the oscillations is, at best, equal to the visibility in the case of the classically driven 2LS. The lower two lines in Fig. 2(c) show the visibility for  $\chi_2 \rightarrow 0$  (dashed black, which corresponds to the visibility of the source 2LS) and  $\chi_2 \rightarrow 1/2$  (red). Note that for the quantum flux, as  $\chi_2 > 1/2$ , the visibility of the oscillations increases again. Finally, we can also fit the visibility lines with Eq. (8), thus finding the extinction coefficient as a function of the  $\chi_2$  parameter; showing that the visibility in the oscillations for the target 2LS and the quantum flux is optimized reaching the limit  $\chi_2 \rightarrow 1$ .

### Time-dependent emission spectra

Beyond the intensity of the light emitted by the 2LS, we now consider the spectral structure of the emission. The time-dependent emission spectra of a 2LS driven with pulses of classical light has been already observed [71, 72, 89, 90], but for completeness, we reproduce it in dashed coloured lines in Fig. 3(b), for pulses of area  $A = n\pi$ , with  $n$  an integer ranging from one to five. Thus, starting from  $A = \pi$  we observe a single line, whose width is compatible with the natural Lorentzian profile of the 2LS (shown in the panel as dotted black lines). However, for large areas we find the following pattern: for areas  $A = 2n\pi$ , there are  $2n - 1$  peaks, namely  $n - 1$  lateral peaks on each side of a central peak, which is developing shoulders. For areas  $A = (2n + 1)\pi$ , these shoulders transition into an additional lateral peak (so, in these cases the emission spectra consists of  $2n + 1$  peaks), and the central peak follows snugly the natural Lorentzian profile of the emitter.

The emission spectra of the target 2LS (which is driven with pulses of quantum rather than classical light) is always given by a single line, which, although has a sub-natural linewidth, it does not have a Lorentzian profile; and it is independent on the pulse area. On the other hand, we find that the emission spectra from the quantum flux inherit their shape from the spectra from the source 2LS, as shown in solid coloured lines in Fig. 3(b). However, despite the similarities between the emission spectra, there are a few details worth mentioning. Firstly, on areas

equal to even multiples of  $\pi$ , the shoulders arising around the central peak are more intense, and overall, the lateral peaks are more intense. The conservation of energy is guaranteed by the fact that the maxima of the central peaks of the quantum flux is vastly reduced (there is a dip in the intensity around the central frequency of the 2LS), as compared to its counterpart for the source 2LS. Finally, we note that the spectra shown in Fig. 3 are independent of the choice of  $\chi_2$  (although,  $\chi_1$  has to be nonzero, otherwise there would be no quantum excitation cascading to the target 2LS), which means that the dynamical spectrum of the pulsed cascaded 2LS is independent of the experimental configuration through which the quantum flux is measured.

### Time-dependent occupation

The population of the source 2LS can be described qualitatively as follows: odd- $\pi$  pulses leave the 2LS in its excited state, followed by the exponential decay associated to the spontaneous emission from the 2LS. Conversely, even- $\pi$  (almost) leave the 2LS in its ground state. However, the latter statement (without the “almost”) is only true in the limit of vanishing short pulses. Beyond that limit, the 2LS is left in a superposition between the excited and ground state, with a larger contribution from the latter. Therefore, in this case one also

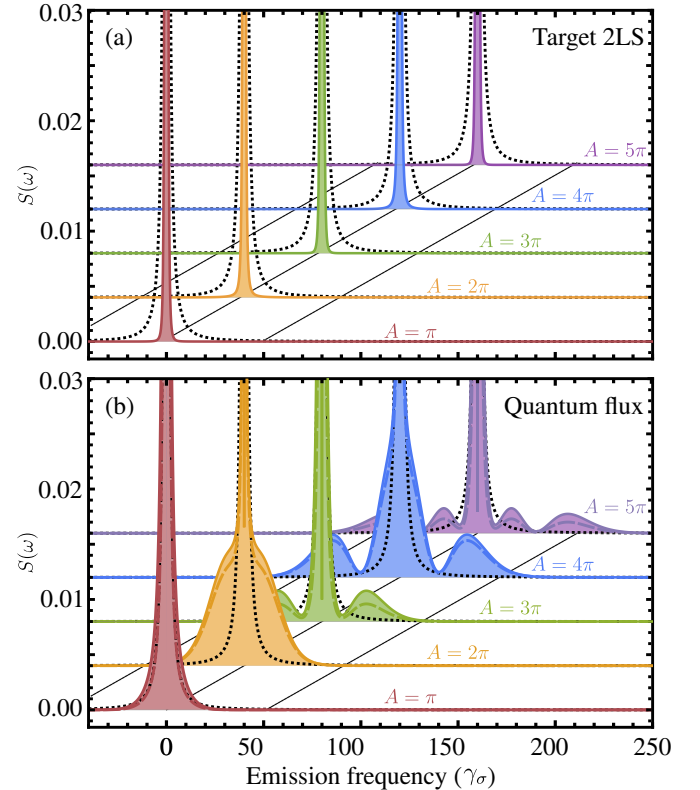


Figure 3. **Time dependent emission spectra for various pulse areas.** (a) Photoluminescence of the 2LS driven with quantum pulses of light. (b) Same as in panel (a) but for the quantum flux (solid) of the system. For completeness, the emission spectra of the source 2LS (dashed). In both panels, the dotted black lines indicate the Lorentzian profile corresponding to the natural linewidth of the emitter.

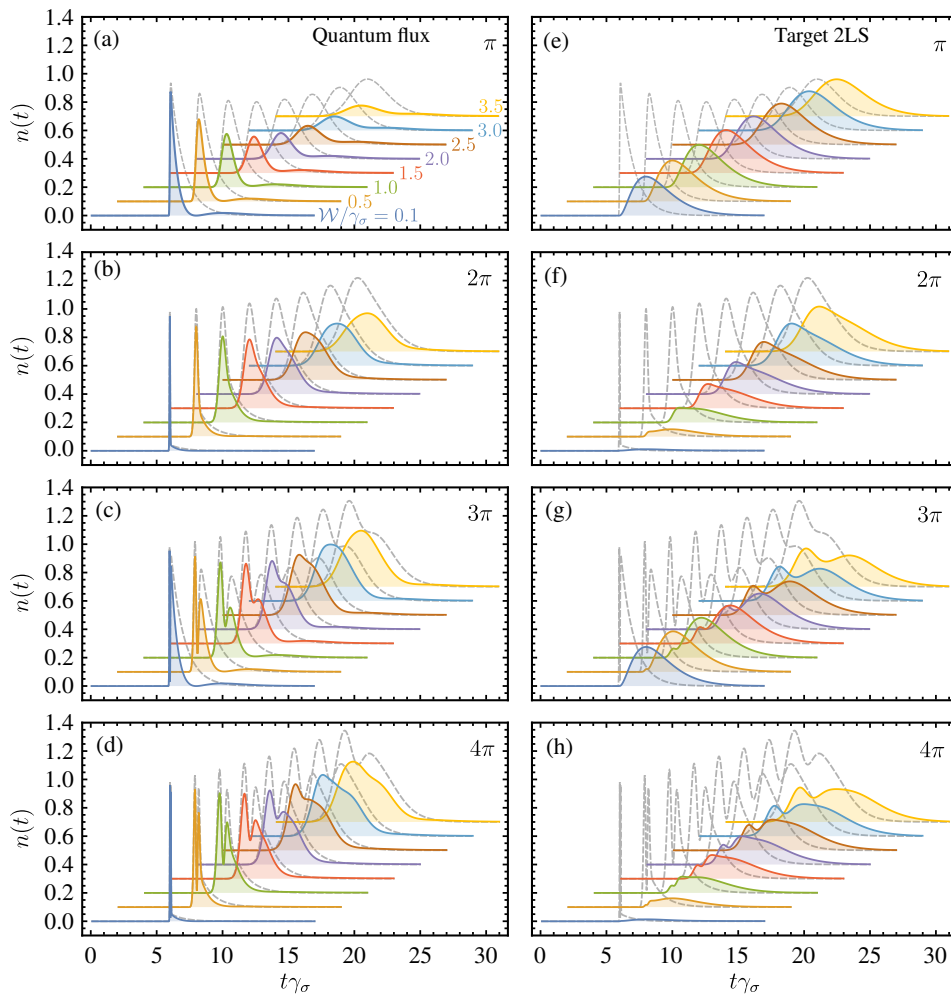


Figure 4. **Occupation of the pulsed emitters.** Comparison between the averaged time-dependent population of the source 2LS (shown as gray dashed lines) and the quantum flux (left column) and the target 2LS (right column), for various key pulse areas (noted on the top right corner of each panel) as a function of the length  $\mathcal{W}$  of the pulse of classical light (shown as the various colours and labelled in panel (a)). For the figure we used  $\chi_2 = 0.5$ .

observes an exponential decay in the occupation of the 2LS after it has interacted with the whole pulse. The behaviour of the time-dependent population of the source 2LS is shown in gray dashed lines in Figs. 4(a-d), for pulses of area  $A = \pi, 2\pi, 3\pi$  and  $4\pi$ , respectively. On each panel, the various lines indicate the variation of the *ideal* shape (i.e., for  $\mathcal{W}/\gamma_\sigma \rightarrow 0$ ) as the length of the pulse increases. For instance, in panel (a) we show that the peaks become smoother, broader and, for pulses longer than the lifetime of the 2LS, they begin to deform. The latter occurs because the pulse is so long, that the 2LS has time to become excited, behave as a photon blockade before emitting a photon, and become excited again from the same pulse. A similar behavior is also observed for pulses of larger areas, with the added effect that then the distance between the maxima of the various peaks increases, while their relative visibility reduces.

The populations for the quantum flux and for the target 2LS are shown as coloured lines in the left and right columns of Fig. 4, respectively. Similarly to the emission spectra, the pop-

ulations for the quantum flux inherit their behaviour from the populations from the source 2LS, again, with notable differences. Firstly, the curves for the quantum flux are less intense, because part of the energy from the source 2LS goes to the target 2LS. Secondly, the populations for the quantum flux display a small, broad peak beyond the *main* features of the populations. Namely, after the pulse is absorbed, the population does not decrease monotonously, but after a few lifetimes, we see a another increase of the population. Such a feature occurs for all pulse areas (cf. the coloured lines in Figs. 4(a-d); although it is more prominent for pulses of areas of odd multiple integers of  $\pi$ ), and it is visible even for the longest pulses considered in this manuscript. Formally, the appearance of the delayed peak is a consequence of the interference between the emission from the source and target 2LSs, which becomes evident when computing the population of the quantum flux  $\text{Tr}\{\rho(t)\mathcal{O}^\dagger\mathcal{O}\}$ , with  $\mathcal{O}$  the operator in Eq. (5). Further, in the occupation of the target 2LS, shown in Figs. 4(e-h), we see a less intense profile with a smoother growth and decay,

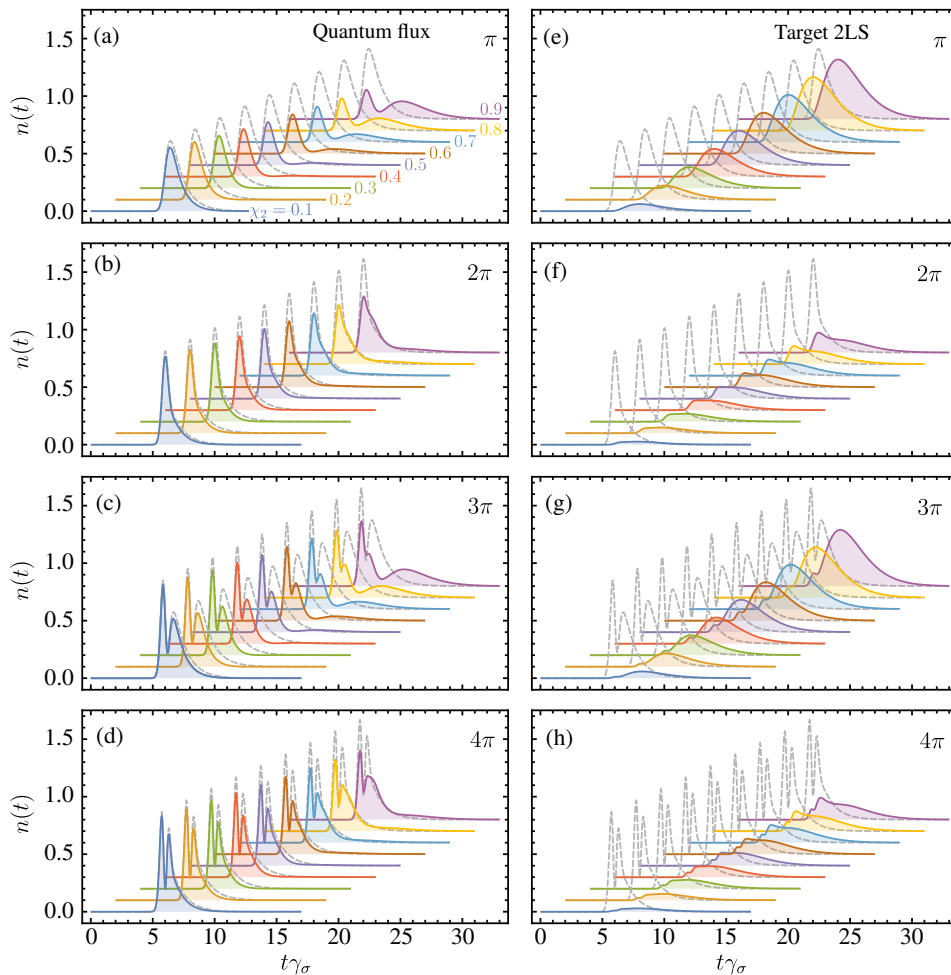


Figure 5. **Variation of the occupation as a function of  $\chi_2$ .** Comparison between the averaged time-dependent population of the source 2LS (shown as gray dashed lines) and the quantum flux (left column) and the target 2LS (right column), for various key pulse areas (noted on the top right corner of each panel), as a function of  $\chi_2$ , that is, the fraction of light that is transferred to the target 2LS (shown as the various colours and labelled in panel (a)). For the figure we used  $\mathcal{W}/\gamma_\sigma = 1$ .

and notably, delayed with respect to the profile observed in the source 2LS and the quantum flux. Figure 5 shows how the populations of the quantum flux and the target 2LS vary as a function of the parameter  $\chi_2$ . For the latter, the effect is mainly an increase of the intensity, as shown in Figs. 5(e–h). Given that  $\chi_2$  gauges how much of the excitation from the source 2LS is redirected to the target 2LS, our observation is not surprising. However, for even- $\pi$  pulses we find that the Rabi oscillations become more prominent as  $\chi_2$  is increased. However, for the populations of the quantum flux, shown in Figs. 5(a–d), we see that, while the shape of the *main* feature of the populations remains unchanged (they are merely damped), the intensity of the secondary peak, arising from by interference between the source and the target 2LS, increases together with the value of  $\chi_2$ . As we shall see in the following section, the appearance of this peak in the quantum flux is a signature of stimulated emission in the system [59].

### Second order correlations

We now discuss the temporal structure of the light, and specifically in the second-order coherence function  $g^{(2)}(0)$  of the

emission. Figure 6 shows the correlation function of the source 2LS (dashed), the quantum flux (solid red) and the target 2LS (solid blue) for three pulse lengths. The figures show the ratio of the correlations between photons emitted during a single pulse and the correlations between photons emitted from different pulses. Namely, the normalization commonly done in pulsed-excitation experiments. On the four panels we can observe a similar behaviour, namely the correlation function obtained with even- $\pi$  pulses is larger than what it is obtained for odd- $\pi$  pulses. However, note that only in Fig. 6(a) the peaks in the correlations for the source 2LS and the quantum flux become bunched; namely, the correlation function becomes larger than 1. As the pulses become broader, the maxima of the correlations, which still occur for pulses of (approximately) even- $\pi$  areas, remain antibunched, i.e., below 1. Thus, even if the emission for, e.g.,  $2\pi$  pulses is expected to be a bunched pair of photons, this is only true in the limit of small pulse lengths. When the latter condition is not fulfilled, the photons pairs are less antibunched than those emitted from, e.g.,  $\pi$ -pulses, but remain antibunched nonetheless. In the limit of

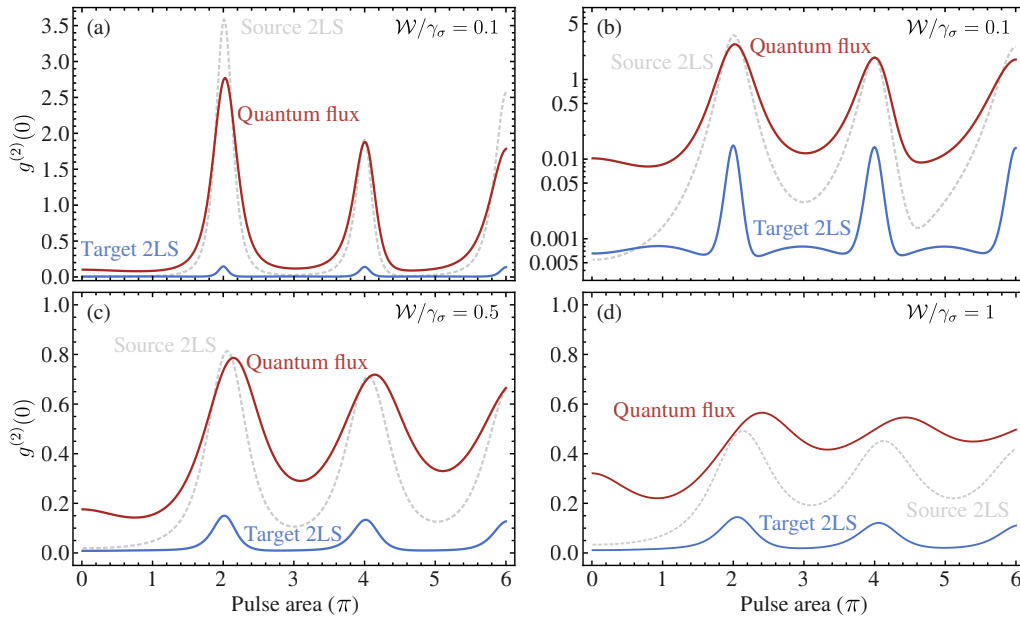


Figure 6. **Second-order coherence function**  $g^{(2)}(0)$ . Comparison of the correlation functions of the source 2LS (dashed gray), the target 2LS (solid blue) and quantum flux (solid red) as a function of the pulse length  $W$ . Namely, (a)  $W/\gamma_\sigma = 0.1$ , (c)  $W/\gamma_\sigma = 0.1$  and (d)  $W/\gamma_\sigma = 0.1$ . Panel (b) shows the same case as panel (a) but in logarithmic scale to reveal the details of the behaviour from the target 2LS.

very long pulses, where the excitation profile becomes essentially flat, we recover the results of cw-excitation: perfect antibunching in the source 2LS, target 2LS and quantum flux. Moreover, in the same way in which the maxima and minima of the Rabi oscillations drift away from integer- $\pi$ -pulses, as the length of the pulses increases, the maxima of correlations also drift away from the even- $\pi$ -pulses; which is specially visible for the case of the quantum flux (cf. panel (d)).

Moreover, we also find that for a large range of pulse areas, the correlation function of the target 2LS always remains more antibunched than the correlation function of both the source 2LS and the quantum flux, in agreement with previous theoretical predictions made on cascaded structures excited with cw-excitation [61]. The range of areas in which the previous affirmation is true increases as the exciting pulses become broader. In fact, already for pulses with  $W/\gamma_\sigma = 0.5$  the target 2LS is *always more antibunched* than the source 2LS. Thus, here we confirm that the method of cascaded excitation can also be used as a mechanism to improve the antibunching in pulsed systems. Finally, we highlight that, for short pulses, the correlation function of the quantum flux is always larger than its counterpart for the source 2LS, except around the vicinity of the even- $\pi$ -pulses, where the relation inverts, in agreement with recent experimental observations [59].

Such an effect can be easily understood further considering the structure of the emission, this time with regards to the delayed correlations, namely the  $g^{(2)}(t_1, t_2)$  function, which relates a pair of photons (not necessarily consecutive) emitted at time  $t_1$  and  $t_2$ , respectively. Thus, we compute a two-photon correlation map that, but instead of considering the frequency of the emitted photons [91–97], we correlate their emission times. Figure 7 shows the delayed correlations of photon pairs

emitted from the source 2LS, the target 2LS and the quantum flux. Although the correlation map from the target 2LS seems to be a copy from the correlations for the source 2LS, the time scales in the two figures are different. In fact, the correlation in the target 2LS decay almost two times as slowly as their counterpart for the source 2LS. Such an observation is also in agreement with the fact that the emission from the target 2LS is also more spread in time, as we showed in Figs. 4 and 5 and discussed in the previous sections. On the other hand, the correlations from the quantum flux are qualitatively different from those of the *bare* 2LS. Instead of the fairly straight correlations lines at  $t_1$  and  $t_2 = 1/\gamma_\sigma$ , we observe the appearance of strong correlations along the diagonal of the figure, that is, for  $t_1 = t_2$ ; namely, we find correlations in pairs of photons emitted simultaneously, which is a signature of *stimulated emission* between just two quanta of light [98]. It is important to keep in mind that the diagonal line appearing on Fig. 7(c), which indicates emission at zero delay, truly indicate simultaneous emission, and it is not equivalent to the results shown in Fig. 6, where the zero delay refers to emission within a single pulse. Furthermore, note that the results shown in Fig. 7 correspond to an excitation pulse of area  $\pi$ , which usually is regarded as a *single photon* excitation pulse. Thus, our results also reveal the Poissonian character of the laser pulse: sometimes, a photon from the pulse excites the 2LS. Later, a subsequent photon from the same pulse, which is only there because of the fluctuations of the photon number in the coherent state of the laser, reaches the now-excited-2LS, which then leads to the generation of two photons sharing the same temporal mode.

The stimulated emission process does not take place only at large intensities. In fact, the quantum flux always displays such a process, even with weak pulses! Figure 8(a) shows the inte-

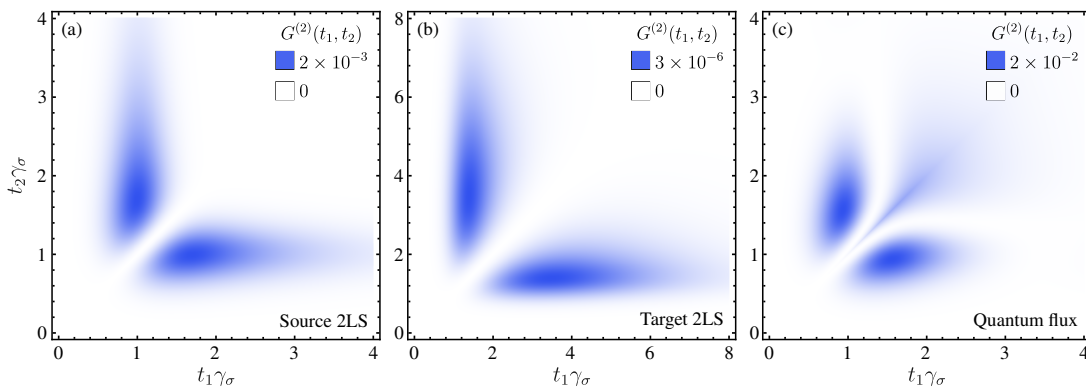


Figure 7. **Time-delayed second-order coherence function**  $G^{(2)}(t_1, t_2)$ . (a) Correlation function for the source 2LS, displaying strong correlations between photons emitted in the close vicinity of the maximum of the excitation pulse. (b) The target 2LS inherits the shape of its correlation from the source 2LS, but although they have the same decay rate  $\gamma_\sigma$ , the correlations of the target 2LS spread further in time and are attenuated by over three orders of magnitude. (c) The quantum flux shows the lobes around the maximum of the excitation pulse, but also displays correlations on the diagonal of the figure, which correspond to photons emitted simultaneously ( $t_1 = t_2$ ) and beyond the lifetime of the 2LS. The figure corresponds to excitation with a  $\pi$ -pulse of length  $\mathcal{W}/\gamma_\sigma = 1$ .

grated correlation function  $\tilde{G}^{(2)} = \int G^{(2)}(t, t) dt$  of the quantum flux, which quantifies the total intensity of the correlations between photon pairs emitted simultaneously. Firstly, it is striking that the system displays same-time correlations even for fairly weak pulses, which indicates that they are not a consequence of the intensity of the pulse, but rather of the quantum interference that originates in the process of the quantum cascaded excitation. Thus, the correlation isolines in Fig. 8(a) are not given by straightforward shapes. Instead they are the result of the complex internal dynamics of excitation and both spontaneous and stimulated emission. The latter is *always* a present element in the dynamics of the quantum flux, because otherwise its same-time correlations would be exactly zero (as it is in the case of the source and target 2LSs). Lastly, in Fig. 8(b) we show various equal-time correlation functions for the quantum flux under  $\pi$ -,  $2\pi$ -,  $3\pi$ - and  $4\pi$ -pulses. Although their specific shape varies as the intensity of the pulse increases, they all share an important fact: after their last peak, the correlations can be perfectly fitted with an exponential function  $G_0 e^{-\gamma_d t}$  with an exponent  $\gamma_d = 2\gamma_\sigma$ . Such a behaviour is true independently of the intensity of the pulse and for short and moderately long pulses. However, for pulses with  $\mathcal{W}/\gamma_\sigma > 4$  the exponent starts to deviate from exactly two and becomes slightly smaller. Nonetheless, we can confirm that except for ultra long pulses, the lifetime (which in general is computed as  $\tau = 1/\gamma$ ) of these correlations is half of the lifetime of the spontaneous emission, i.e.,  $\tau_d = \tau_\sigma/2$ , which is in agreement with recent experimental observations [59].

## DISCUSSION

Based on recent experimental results [59], we have presented a thorough theoretical description of the dynamics of a quantum system excited with the quantum emission from a pulsed source of quantum light. Thus, we have used two of the most fundamental, yet phenomenologically rich, quantum

system available, a 2LS, as the source and the optical target of the quantum light. Firstly, we showed that the expected Rabi oscillations in the total emission, predicted from the pulse area theorem, are well visible only when the length of the driving pulse is significantly shorter than the lifetime of the 2LS. When the latter condition is not met, the visibility of the oscillations start to decrease down to the point in which one cannot longer speak of oscillations, as the intensity of the emission increases monotonically. Furthermore, we found that the maxima and minima of the Rabi oscillations are given exactly by even- and odd- $\pi$ -pulses, respectively. However, such an expectation is only met in the limit of ultra-short pulses, and the position of the maxima and minima drift away as the length of the pulse increases. This is an important fact that experimentalist should bear in mind when performing these types of measurements, where the intensity of the pulse is not known *a priori*, but instead is fitted through the position of the first maximum (corresponding to a  $\pi$ -pulse) and minimum (corresponding to a  $2\pi$ -pulse).

Continuing with the single-particle observables, we found that both the time-dependent spectrum and the occupation the source 2LS are inherited closely by the quantum flux. Thus, we have observed the appearance of lateral peaks around the central peak of emission, and gave the positions at which those lateral peaks are located. On the other hand, we found that the emission spectra of the target 2LS is *always* given by a single line, with a narrower profile than its natural linewidth. A closer inspection into at the occupation of the target 2LS and the quantum flux, revealed that a considerable part of the light is emitted well beyond the limits of one lifetime of the 2LS.

The relevance of such a delayed emission is unveiled when considering the two-particles observables, namely the second-order coherence function. The quantum flux displays strong correlations between photons emitted simultaneously, which is an indication of stimulated emission from the system. Such an observation is supported by the fact that, firstly they are not present in the correlations of the source nor the target



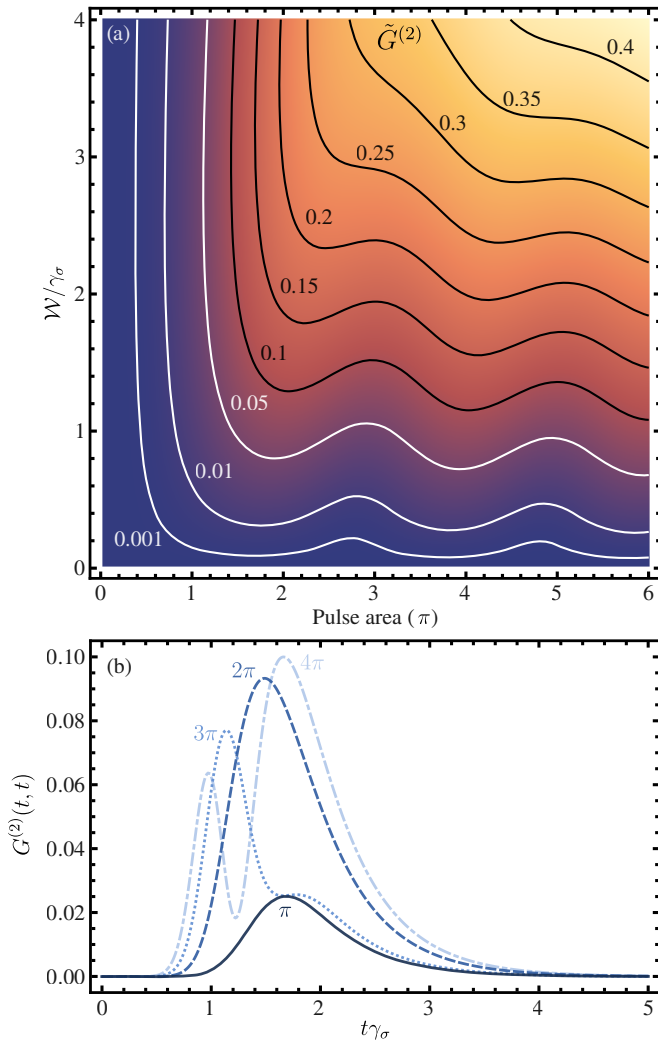


Figure 8. **Signatures of stimulated emission on the  $G^{(2)}(t, t)$  of the quantum flux.** (a) Integrated equal-time correlation function,  $\tilde{G}^{(2)} = \int G^{(2)}(t, t) dt$ , of the quantum flux as a function of the length and intensity of the driving pulse. Even with intensities below  $\pi$ -pulses, we find that there same-time correlations indicating stimulated emission. (b) Equal-time correlation function for various intensities. In all the cases, after the last peak, the correlations decay with an exponent  $\gamma_d = 2\gamma_\sigma$ . Panel (a) was obtained with  $\chi_2 = 1/2$ , but choosing a different parameter only rescales the figure and does not changes its shape. Panel (b) was obtained with a pulse of length  $\mathcal{W}/\gamma_\sigma = 1$ ,  $\chi_2 = 1/2$  and pulse area as indicated next to each line.

2LSs, and secondly the lifetime of these correlations is exactly half the lifetime of the spontaneously emitted photons. Finally, we also found that the light emitted from the target 2LS is always more antibunched than the emission from the source 2LS. Thus, together with the observation of its spectrum, we demonstrated that, even under pulsed excitation, the quantum cascaded excitation can be used as a mechanism to produce subnatural linewidth antibunched light, as shown in Ref. [61, 99] for continuous coherent driving.

The approach used here, namely, the consideration of pulsed rather than continuous excitation, makes our results accessible to realization with state-of-the-art setups. Thus, we believe that our results can be used as a guideline to the exploration of quantum phenomena arising in condensed matter physics, and working towards the resolution of both fundamental and practical questions. For instance, the quantum flux emission is a natural resource that can be used to exploit quantum interferences and develop, e.g., mechanisms akin to homodyne detection, or two-photon interference protocols. Alternatively, starting from the results form the target 2LS, we can envisage a mechanism to generate *more antibunched* photons emitted with narrower line. In fact, such a mechanism could be constructed in a cascaded scheme, and then one should consider up to which point the emission remains to be coherent, and whether the emission line continues to reduce. Furthermore, a natural continuation for this work would be to include chirping [100] into the description of the pulse, or to consider other types of quantum light as the source of excitation. For instance, photon streams with a varying coherence function (which could be used as an spectroscopy tool) or other types of quantum correlations, including entanglement.

#### DATA AVAILABILITY STATEMENT

The data that support the plots within this paper and other findings of this study are available from the corresponding Author upon reasonable request.

#### CODE AVAILABILITY

The various codes used for modelling the data are available from the corresponding Author upon reasonable request.

#### ACKNOWLEDGEMENTS

This research was funded in whole by the Polish National Science Center (NCN) ‘‘Sonatina’’ project CARMEL with number 2021/40/C/ST2/00155. For the purpose of Open Access, the authors have applied CC-BY public copyright licence to any Author Accepted Manuscript (AAM) version arising from this submission.

#### AUTHOR CONTRIBUTIONS

The Author confirms the sole responsibility for the conception of the study, presented results and manuscript preparation.

#### COMPETING INTERESTS

The Author declares no competing interests.

- 
- [1] A. Einstein, Concerning an Heuristic Point of View Toward the Emission and Transformation of Light, *Annalen der Physik* **17**, 132 (1905).
- [2] A. Einstein, Zur Quantentheorie der Strahlung, *Physika Zeitschrift* **18**, 121 (1917).
- [3] D. Browne, S. Bose, F. Mintert, and M. Kim, From quantum optics to quantum technologies, *Progress in Quantum Electronics* **54**, 2 (2017).
- [4] R. Gutzler, M. Garg, C. R. Ast, K. Kuhnke, and K. Kern, Light–matter interaction at atomic scales, *Nature Reviews Physics* **3**, 441 (2021).
- [5] A. González-Tudela, A. Reiserer, J. J. García-Ripoll, and F. J. García-Vidal, Light–matter interactions in quantum nanophotonic devices, *Nature Reviews Physics* **6**, 166 (2024).
- [6] B. Wang, M. Aidelsburger, J. Dalibard, A. Eckardt, and N. Goldman, Cold-Atom Elevator: From Edge-State Injection to the Preparation of Fractional Chern Insulators, *Physical Review Letters* **132**, 163402 (2024).
- [7] T. Langen, G. Valtolina, D. Wang, and J. Ye, Quantum state manipulation and cooling of ultracold molecules, *Nature Physics* **20**, 702 (2024).
- [8] J. R. Williams, C. A. Sackett, H. Ahlers, D. C. Aveline, P. Boegel, S. Botsi, E. Charron, E. R. Elliott, N. Gaaloul, E. Giese, W. Herr, J. R. Kellogg, J. M. Kohel, N. E. Lay, M. Meister, G. Müller, H. Müller, K. Oudrhiri, L. Phillips, A. Pichery, E. M. Rasel, A. Roura, M. Sbroscia, W. P. Schleich, C. Schneider, C. Schubert, B. Sen, R. J. Thompson, and N. P. Bigelow, Pathfinder experiments with atom interferometry in the Cold Atom Lab onboard the International Space Station, *Nature Communications* **15**, 6414 (2024).
- [9] C. Weisbuch, M. Nishioka, A. Ishikawa, and Y. Arakawa, Observation of the Coupled Exciton-Photon Mode Splitting in a Semiconductor Quantum Microcavity, *Phys. Rev. Lett.* **69**, 3314 (1992).
- [10] F. Riminucci, A. Gianfrate, D. Nigro, V. Ardizzone, S. Dhuey, L. Francaviglia, K. Baldwin, L. N. Pfeiffer, D. Ballarini, D. Trypogeorgos, A. Schwartzberg, D. Gerace, and D. Sanvitto, Polariton Condensation in Gap-Confined States of Photonic Crystal Waveguides, *Physical Review Letters* **131**, 246901 (2023).
- [11] H. Li, F. Chen, H. Jia, Z. Ye, H. Zhou, S. Luo, J. Shi, Z. Sun, H. Xu, H. Xu, T. Byrnes, Z. Chen, and J. Wu, All-optical temporal logic gates in localized exciton polaritons, *Nature Photonics* **18**, 864 (2024).
- [12] M. Makhonin, A. Delphan, K. W. Song, P. Walker, T. Isoniemi, P. Claronino, K. Orfanakis, S. K. Rajendran, H. Ohadi, J. Heckötter, M. Assmann, M. Bayer, A. Tartakovskii, M. Skolnick, O. Kyriienko, and D. Krizhanovskii, Nonlinear Rydberg exciton-polaritons in Cu<sub>2</sub>O microcavities, *Light: Science & Applications* **13**, 47 (2024).
- [13] W. Wen, J. Liang, H. Xu, F. Jin, Y. G. Rubo, T. C. H. Liew, and R. Su, Trembling Motion of Exciton Polaritons Close to the Rashba-Dresselhaus Regime, *Physical Review Letters* **133**, 116903 (2024).
- [14] T. Wang, H. Sun, X. Li, and L. Zhang, Chiral Phonons: Prediction, Verification, and Application, *Nano Letters* **24**, 4311 (2024).
- [15] J. Yan, R. Shi, J. Wei, Y. Li, R. Qi, M. Wu, X. Li, B. Feng, P. Gao, N. Shibata, and Y. Ikuhara, Nanoscale Localized Phonons at Al<sub>2</sub>O<sub>3</sub> Grain Boundaries, *Nano Letters* **24**, 3323 (2024).
- [16] M. Mo, A. Tamm, E. Metsanurk, Z. Chen, L. Wang, M. Frost, N. J. Hartley, F. Ji, S. Pandolfi, A. H. Reid, P. Sun, X. Shen, Y. Wang, X. Wang, S. Glenzer, and A. A. Correa, Direct observation of strong momentum-dependent electron-phonon coupling in a metal, *Science Advances* **10**, eadk9051 (2024).
- [17] M. Hong, R. B. Dawkins, B. Bertoni, C. You, and O. S. Magaña-Loaiza, Nonclassical near-field dynamics of surface plasmons, *Nature Physics* **20**, 830 (2024).
- [18] A. Stefanu, N. J. Halas, P. Nordlander, and E. Cortes, Electronic excitations at the plasmon–molecule interface, *Nature Physics* **20**, 1065 (2024).
- [19] C. J. Sánchez Martínez, J. Feist, and F. J. García-Vidal, A mixed perturbative-nonperturbative treatment for strong light-matter interactions, *Nanophotonics* **13**, 2669 (2024).
- [20] T. Wu, C. Wang, G. Hu, Z. Wang, J. Zhao, Z. Wang, K. Chaykun, L. Liu, M. Chen, D. Li, S. Zhu, Q. Xiong, Z. Shen, H. Gao, F. J. Garcia-Vidal, L. Wei, Q. J. Wang, and Y. Luo, Ultrastrong exciton-plasmon couplings in WS<sub>2</sub> multilayers synthesized with a random multi-singular metasurface at room temperature, *Nature Communications* **15**, 3295 (2024).
- [21] F. Borsoi, N. W. Hendrickx, V. John, M. Meyer, S. Motz, F. Van Riggelen, A. Sammak, S. L. De Snoo, G. Scappucci, and M. Veldhorst, Shared control of a 16 semiconductor quantum dot crossbar array, *Nature Nanotechnology* **19**, 21 (2024).
- [22] J. Mondal, R. Lamba, Y. Yukta, R. Yadav, R. Kumar, B. Pani, and B. Singh, Advancements in semiconductor quantum dots: Expanding frontiers in optoelectronics, analytical sensing, biomedicine, and catalysis, *Journal of Materials Chemistry C* **12**, 10330 (2024).
- [23] E. K. Vishnu, E. M. Thomas, L. Prasad, and K. G. Thomas, Trap States in Semiconductor Quantum Dots: Friends or Foes, *The Journal of Physical Chemistry C* **128**, 4373 (2024).
- [24] C. Spinnler, G. N. Nguyen, Y. Wang, L. Zhai, A. Javadi, M. Erbe, S. Scholz, A. D. Wieck, A. Ludwig, P. Lodahl, L. Midolo, and R. J. Warburton, A single-photon emitter coupled to a phononic-crystal resonator in the resolved-sideband regime, *Nature Communications* **15**, 9509 (2024).
- [25] M. Kędziora, A. Opala, R. Mastroia, L. De Marco, M. Król, K. Łempicka-Mirek, K. Tyska, M. Ekielski, M. Guziewicz, K. Bogdanowicz, A. Szerling, H. Sigurdsson, T. Czyszanowski, J. Szczytko, M. Matuszewski, D. Sanvitto, and B. Piętka, Predesigned perovskite crystal waveguides for room-temperature exciton–polariton condensation and edge lasing, *Nature Materials* **23**, 1515 (2024).
- [26] A. Fieramosca, R. Mastroia, K. Dini, L. Dominici, L. Polimeno, M. Pugliese, C. T. Prontera, L. De Marco, V. Maiorano, F. Todisco, D. Ballarini, M. De Giorgi, G. Gigli, T. C. H. Liew, and D. Sanvitto, Origin of Exciton–Polariton Interactions and Decoupled Dark States Dynamics in 2D Hybrid Perovskite Quantum Wells, *Nano Letters* **24**, 8240 (2024).
- [27] M. A. Masharin, T. Oskolkova, F. Isik, H. Volkan Demir, A. K. Samusev, and S. V. Makarov, Giant Ultrafast All-Optical Modulation Based on Exceptional Points in Exciton–Polariton Perovskite Metasurfaces, *ACS Nano* **18**, 3447 (2024).
- [28] S.-C. An, Y. Lim, K. Y. Lee, D. Choi, S. Kim, S.-H. Gong, J. W. Yoon, and Y. C. Jun, Topological Exciton Polaritons in Compact Perovskite Junction Metasurfaces, *Advanced Functional Materials* **34**, 2313840 (2024).
- [29] J. Zhao, A. Fieramosca, K. Dini, R. Bao, W. Du, R. Su, Y. Luo, W. Zhao, D. Sanvitto, T. C. H. Liew, and Q. Xiong, Exciton polariton interactions in Van der Waals superlattices at room

- temperature, *Nature Communications* **14**, 1512 (2023).
- [30] M. Król, K. Łempicka-Mirek, K. Rechcińska, M. Furman, K. Nogajewski, R. Mazur, P. Morawiak, W. Piecek, W. Pacuski, J. Szczytko, and B. Piętka, Universality of open microcavities for strong light-matter coupling, *Optical Materials Express* **13**, 2651 (2023).
- [31] M.-S. Hwang and H.-G. Park, Manipulating the nonlinearity of transition-metal dichalcogenide polaritons, *Light: Science & Applications* **12**, 275 (2023).
- [32] J. K. König, J. M. Fitzgerald, J. Hagel, D. Erkensten, and E. Malic, Interlayer exciton polaritons in homobilayers of transition metal dichalcogenides, *2D Materials* **10**, 025019 (2023).
- [33] K. Shen, K. Sun, M. F. Gelin, and Y. Zhao, Cavity-Tuned Exciton Dynamics in Transition Metal Dichalcogenides Monolayers, *Materials* **17**, 4127 (2024).
- [34] M. D. Fraser, Coherent exciton-polariton devices, *Semiconductor Science and Technology* **32**, 093003 (2017).
- [35] M. Król, K. Rechcińska, K. Nogajewski, M. Grzeszczyk, K. Łempicka, R. Mirek, S. Piotrowska, K. Watanabe, T. Taniguchi, M. R. Molas, M. Potemski, J. Szczytko, and B. Piętka, Exciton-polaritons in multilayer WSe<sub>2</sub> in a planar microcavity, *2D Materials* **7**, 015006 (2019).
- [36] P. Ninhos, C. Tserkezis, N. A. Mortensen, and N. M. R. Peres, Tunable Exciton Polaritons in Band-Gap Engineered Hexagonal Boron Nitride, *ACS Nano* **18**, 20751 (2024).
- [37] H. S. Lee, J. Sung, D.-J. Shin, and S.-H. Gong, The impact of hBN layers on guided exciton-polariton modes in WS<sub>2</sub> multilayers, *Nanophotonics* **13**, 1475 (2024).
- [38] H. J. Kimble, M. Dagenais, and L. Mandel, Photon Antibunching in Resonance Fluorescence, *Phys. Rev. Lett.* **39**, 691 (1977).
- [39] P. A. Apanasevich and S. Y. Kilin, Photon Bunching and Antibunching in Resonance Fluorescence, *J. Phys. B.: At. Mol. Phys.* **12**, L83 (1979).
- [40] R. Loudon and P. Knight, Squeezed Light, *Journal of Modern Optics* **34**, 709 (1987).
- [41] A. M. Fox, J. J. Baumberg, M. Dabbicco, B. Huttner, and J. F. Ryan, Squeezed Light Generation in Semiconductors, *Phys. Rev. Lett.* **74**, 1728 (1995).
- [42] C. Orzel, A. K. Tuchman, M. L. Fenselau, M. Yasuda, and M. A. Kasevich, Squeezed States in a Bose-Einstein Condensate, *Science* **291**, 2386 (2001).
- [43] Y. Zhang, M. Menotti, K. Tan, V. D. Vaidya, D. H. Mahler, L. G. Helt, L. Zatti, M. Liscidini, B. Morrison, and Z. Vernon, Squeezed light from a nanophotonic molecule, *Nature Communications* **12**, 2233 (2021).
- [44] Z. Wang, Z. Zhan, A. N. Vetlugin, J.-Y. Ou, Q. Liu, Y. Shen, and X. Fu, Structured light analogy of quantum squeezed states, *Light: Science & Applications* **13**, 297 (2024).
- [45] P. G. Kwiat, E. Waks, A. G. White, I. Appelbaum, and P. H. Eberhard, Ultrabright Source of Polarization-Entangled Photons, *Phys. Rev. A* **60**, 773R (1999).
- [46] J. B. Altepeter, E. R. Jeffrey, and P. G. Kwiat, Phase-compensated ultra-bright source of entangled photons, *Optics Express* **13**, 8951 (2005).
- [47] R. M. Stevenson, R. J. Young, P. Atkinson, K. Cooper, D. A. Ritchie, and A. J. Shields, A Semiconductor Source of Triggered Entangled Photon Pairs, *Nature* **439**, 179 (2006).
- [48] A. Dousse, J. Suffczyński, A. Beveratos, O. Krebs, A. Lemaître, I. Sagnes, J. Bloch, P. Voisin, and P. Senellart, Ultrabright Source of Entangled Photon Pairs, *Nature* **466**, 217 (2010).
- [49] R. Trotta, J. Martín-Sánchez, J. S. Wildmann, G. Piredda, M. Reindl, C. Schimpf, E. Zallo, S. Stroj, J. Edlinger, and A. Rastelli, Wavelength-tunable sources of entangled photons interfaced with atomic vapours, *Nature Communications* **7**, 10375 (2016).
- [50] J. C. López Carreño, S. Bermúdez Feijoo, and M. Stobińska, Entanglement in Resonance Fluorescence, *npj Nanophoton.* **1**, 3 (2024).
- [51] A. Kuhn, M. Hennrich, and G. Rempe, Deterministic Single-Photon Source for Distributed Quantum Networking, *Physical Review Letters* **89**, 067901 (2002).
- [52] O. Gazzano, M. de Vasconcellos, C. Arnold, A. Nowak, E. Galopin, I. Sagnes, L. Lanco, A. Lemaître, and P. Senellart, Bright Solid-State Sources of Indistinguishable Single Photons, *Nat. Comm.* **4**, 1425 (2012).
- [53] S. L. Portalupi, G. Hornecker, V. Giesz, T. Grange, A. Lemaître, J. Demory, I. Sagnes, N. D. Lanzillotti-Kimura, L. Lanco, A. Auffèves, and P. Senellart, Bright Phonon-Tuned Single-Photon Source, *Nano Lett.* **15**, 6290 (2015).
- [54] N. Somaschi, V. Giesz, L. D. Santis, J. C. Loredó, M. P. Almeida, G. Hornecker, S. L. Portalupi, T. Grange, C. Antón, J. Demory, C. Gómez, I. Sagnes, N. D. Lanzillotti-Kimura, A. Lemaître, A. Auffèves, A. G. White, L. Lanco, and P. Senellart, Near-Optimal Single-Photon Sources in the Solid State, *Nat. Photon.* **10**, 340 (2016).
- [55] J. C. Loredó, N. A. Zakaria, N. Somaschi, C. Anton, L. D. Santis, V. Giesz, T. Grange, M. A. Broome, O. Gazzano, G. Coppola, I. Sagnes, A. Lemaître, A. Auffèves, P. Senellart, M. P. Almeida, and A. G. White, Scalable Performance in Solid-State Single-Photon Sources, *Optica* **3**, 433 (2016).
- [56] P. Senellart, G. Solomon, and A. White, High-Performance Semiconductor Quantum-Dot Single-Photon Sources, *Nat. Nanotech.* **12**, 1026 (2017).
- [57] R. Uppu, F. T. Pedersen, Y. Wang, C. T. Olesen, C. Papon, X. Zhou, L. Midolo, S. Scholz, A. D. Wieck, A. Ludwig, and P. Lodahl, Scalable integrated single-photon source, *Science Advances* **6**, eabc8268 (2020).
- [58] C. Sánchez Muñoz, E. del Valle, A. González-Tudela, K. Müller, S. Lichtmanecker, M. Kaniber, C. Tejedor, J. J. Finley, and F. P. Laussy, Emitters of N-photon bundles, *Nature Photonics* **8**, 550 (2014).
- [59] L. M. Hansen, F. Giorgino, L. Jehle, L. Carosini, J. C. López Carreño, I. Arrazola, P. Walther, and J. C. Loredó, Non-classical excitation of a solid-state quantum emitter, arXiv:2407.20936 (2024), arXiv:2407.20936.
- [60] J. C. López Carreño and F. P. Laussy, Excitation with Quantum Light. I. Exciting a Harmonic Oscillator, *Phys. Rev. A* **94**, 063825 (2016).
- [61] J. C. López Carreño, C. Sánchez Muñoz, E. del Valle, and F. P. Laussy, Excitation with Quantum Light. II. Exciting a Two-Level System, *Phys. Rev. A* **94**, 063826 (2016).
- [62] S. Mukamel, M. Freyberger, W. Schleich, M. Bellini, A. Zavatta, G. Leuchs, C. Silberhorn, R. W. Boyd, L. L. Sánchez-Soto, A. Stefanov, M. Barbieri, A. Paterova, L. Krivitsky, S. Shwartz, K. Tamasaku, K. Dorfman, F. Schlawin, V. Sandoghdar, M. Raymer, A. Marcus, O. Varnavski, T. Goodson, Z.-Y. Zhou, B.-S. Shi, S. Asban, M. Scully, G. Agarwal, T. Peng, A. V. Sokolov, Z.-D. Zhang, M. S. Zubairy, I. A. Vartanyants, E. del Valle, and F. Laussy, Roadmap on quantum light spectroscopy, *J. Phys. B: At. Mol. Opt. Phys.* **53**, 072002 (2020).
- [63] P. Michler, A. Kiraz, C. Becher, W. V. Schoenfeld, P. M. Petroff, L. Zhang, E. Hu, and A. Imamoglu, A Quantum Dot Single-Photon Turnstile Device, *Science* **290**, 2282 (2000).
- [64] M. Aßmann, F. Veit, J.-S. Tempel, T. Berstermann, H. Stolz, M. Van Der Poel, J. M. Hvam, and M. Bayer, Measuring the

- dynamics of second-order photon correlation functions inside a pulse with picosecond time resolution, *Optics Express* **18**, 20229 (2010).
- [65] A. Reinhard, T. Volz, M. Winger, A. Badolato, K. J. Hennessy, E. L. Hu, and A. İmamoğlu, Strongly Correlated Photons on a Chip, *Nat. Photon.* **6**, 93 (2012).
- [66] D. Zhu, C. Chen, M. Yu, L. Shao, Y. Hu, C. J. Xin, M. Yeh, S. Ghosh, L. He, C. Reimer, N. Sinclair, F. N. C. Wong, M. Zhang, and M. Lončar, Spectral control of nonclassical light pulses using an integrated thin-film lithium niobate modulator, *Light Sci Appl* **11**, 327 (2022).
- [67] M. Karpiński, A. O. C. Davis, F. Soñnicki, V. Thiel, and B. J. Smith, Control and Measurement of Quantum Light Pulses for Quantum Information Science and Technology, *Adv Quantum Tech* **4**, 2000150 (2021).
- [68] F. Soñnicki, M. Miłojajczyk, A. Golestani, and M. Karpiński, Interface between picosecond and nanosecond quantum light pulses, *Nat. Photon.* **17**, 761 (2023).
- [69] S. C. Wein, J. C. Loredó, M. Maffei, P. Hilaire, A. Harouri, N. Somaschi, A. Lemaître, I. Sagnes, L. Lanco, O. Krebs, A. Auffèves, C. Simon, P. Senellart, and C. Antón-Solanas, Photon-number entanglement generated by sequential excitation of a two-level atom, *Nat. Photon.* **16**, 374 (2022).
- [70] F. Albarelli, E. Bisketzi, A. Khan, and A. Datta, Fundamental limits of pulsed quantum light spectroscopy: Dipole moment estimation, *Phys. Rev. A* **107**, 062601 (2023).
- [71] K. A. Fischer, K. Müller, A. Rundquist, T. Sarmiento, A. Y. Piggott, Y. A. Kelaita, C. Dory, K. G. Lagoudakis, K. Müller, and J. Vučković, Self-Homodyne Measurement of a Dynamic Mollow Triplet in the Solid State, *Nat. Photon.* **10**, 163 (2016).
- [72] K. A. Fischer, L. Hanschke, J. Wierzbowski, T. Simmet, C. Dory, J. J. Finley, J. Vučković, and K. Müller, Signatures of Two-Photon Pulses from a Quantum Two-Level System, *Nat. Phys.* **4**, 649 (2017).
- [73] J. A. Smyder, A. R. Amori, M. Y. Odoi, H. A. Stern, J. J. Peterson, and T. D. Krauss, The influence of continuous vs. pulsed laser excitation on single quantum dot photophysics, *Phys. Chem. Chem. Phys.* **16**, 25723 (2014).
- [74] V. Astapenko, T. Bergaliyev, and S. Sakhno, Pulsed excitation of a quantum oscillator: A model accounting for damping, *Open Physics* **22**, 20230208 (2024).
- [75] C. Gustin and S. Hughes, Efficient Pulse-Excitation Techniques for Single Photon Sources from Quantum Dots in Optical Cavities, *Adv Quantum Tech* **3**, 1900073 (2020).
- [76] C. W. Gardiner, Driving a Quantum System with the Output Field from Another Driven Quantum System, *Phys. Rev. Lett.* **70**, 2269 (1993).
- [77] H. J. Carmichael, Quantum Trajectory Theory for Cascaded Open Systems, *Phys. Rev. Lett.* **70**, 2273 (1993).
- [78] J. C. López Carreño, C. Sánchez Muñoz, D. Sanvitto, E. del Valle, and F. P. Laussy, Exciting Polaritons with Quantum Light, *Phys. Rev. Lett.* **115**, 196402 (2015).
- [79] C. A. Downing, J. C. López Carreño, F. P. Laussy, E. del Valle, and A. I. Fernández-Domínguez, Quasichiral Interactions between Quantum Emitters at the Nanoscale, *Phys. Rev. Lett.* **122**, 057401 (2019).
- [80] K. Sun and W. Yi, Chiral state transfer under dephasing, *Physical Review A* **108**, 013302 (2023).
- [81] B. Tissot and G. Burkard, Efficient high-fidelity flying qubit shaping, *Physical Review Research* **6**, 013150 (2024).
- [82] Y. Xiang, S. Cheng, Q. Gong, Z. Ficek, and Q. He, Quantum Steering: Practical Challenges and Future Directions, *PRX Quantum* **3**, 030102 (2022).
- [83] S. Ghosh, A. Opala, M. Matuszewski, T. Paterek, and T. C. H. Liew, Quantum reservoir processing, *npj Quantum Information* **5**, 35 (2019).
- [84] S. Ghosh, A. Opala, M. Matuszewski, T. Paterek, and T. C. H. Liew, Reconstructing Quantum States With Quantum Reservoir Networks, *IEEE Transactions on Neural Networks and Learning Systems* **32**, 3148 (2021).
- [85] J. Dudas, B. Carles, E. Plouet, F. A. Mizrahi, J. Grollier, and D. Marković, Quantum reservoir computing implementation on coherently coupled quantum oscillators, *npj Quantum Information* **9**, 64 (2023).
- [86] A. H. Kiilerich and K. Mølmer, Input-Output Theory with Quantum Pulses, *Phys. Rev. Lett.* **123**, 123604 (2019).
- [87] A. H. Kiilerich and K. Mølmer, Quantum interactions with pulses of radiation, *Phys. Rev. A* **102**, 023717 (2020).
- [88] L. Allen and J. H. Eberly, *Optical Resonance and Two-Level Atoms* (Dover, 1987).
- [89] L. Masters, X.-X. Hu, M. Cordier, G. Maron, L. Pache, A. Rauschenbeutel, M. Schemmer, and J. Volz, On the simultaneous scattering of two photons by a single two-level atom, *Nat. Phot.* **17**, 972 (2023).
- [90] K. Boos, S. K. Kim, T. Bracht, F. Sbresny, J. M. Kaspari, M. Cygorek, H. Riedl, F. W. Bopp, W. Rauhaus, C. Calcagno, J. J. Finley, D. E. Reiter, and K. Müller, Signatures of Dynamically Dressed States, *Phys. Rev. Lett.* **132**, 053602 (2024).
- [91] E. del Valle, A. González-Tudela, F. P. Laussy, C. Tejedor, and M. J. Hartmann, Theory of Frequency-Filtered and Time-Resolved N-Photon Correlations, *Phys. Rev. Lett.* **109**, 183601 (2012).
- [92] B. Piętka, J. Suffczyński, M. Goryca, T. Kazimierczuk, A. Golnik, P. Kossacki, A. Wyszomolek, J. A. Gaj, R. Stepniowski, and M. Potemski, Photon correlation studies of charge variation in a single GaAlAs quantum dot, *Phys. Rev. B* **87**, 035310 (2013).
- [93] A. González-Tudela, F. P. Laussy, C. Tejedor, M. J. Hartmann, and E. del Valle, Two-Photon Spectra of Quantum Emitters, *New J. Phys.* **15**, 033036 (2013).
- [94] M. Peiris, B. Petrak, K. Konthasinghe, Y. Yu, Z. C. Niu, and A. Muller, Two-Color Photon Correlations of the Light Scattered by a Quantum Dot, *Phys. Rev. B* **91**, 195125 (2015).
- [95] B. Silva, C. Sánchez Muñoz, D. Ballarini, A. González-Tudela, M. de Giorgi, G. Gigli, K. West, L. Pfeiffer, E. del Valle, D. Sanvitto, and F. P. Laussy, The Colored Hanbury Brown-Twiss Effect, *Sci. Rep.* **6**, 37980 (2016).
- [96] J. C. López Carreño, E. del Valle, and F. P. Laussy, Photon Correlations from the Mollow Triplet, *Laser Photon. Rev.* **11**, 1700090 (2017).
- [97] J. C. López Carreño, E. del Valle, and F. P. Laussy, Frequency-Resolved Monte Carlo, *Sci. Rep.* **8**, 6975 (2018).
- [98] E. Rephaeli and S. Fan, Stimulated Emission from a Single Excited Atom in a Waveguide, *Phys. Rev. Lett.* **108**, 143602 (2012).
- [99] J. C. López Carreño, E. Zubizarreta Casalengua, F. P. Laussy, and E. del Valle, Joint Subnatural-Linewidth and Single-Photon Emission from Resonance Fluorescence, *Quantum Sci. Technol.* **3**, 045001 (2018).
- [100] F. Kappe, Y. Karli, G. Wilbur, R. G. Krämer, S. Ghosh, R. Schwarz, M. Kaiser, T. K. Bracht, D. E. Reiter, S. Nolte, K. C. Hall, G. Weihs, and V. Remesh, Chirped Pulses Meet Quantum Dots: Innovations, Challenges, and Future Perspectives, *Adv Quantum Tech* **3**, 2300352 (2024).